Structure of Medium-Scale Atmospheric Waves in the Southern Hemisphere Summer

WILLIAM J. RANDEL AND JOHN L. STANFORD

Department of Physics, Iowa State University, Ames 50011

25 October 1982 and 6 May 1983

ABSTRACT

Recently reported medium-scale wave dominance of the Southern Hemisphere summer circulation is studied using NMC geopotential height fields for the 1978–79 summer. These features, corroborated by independent analyses of satellite microwave measurements, are apparent in meridional thermal winds derived from the NMC grids.

In the time mean, we observe strong medium-scale waves which extend throughout the troposphere and lower stratosphere, in agreement with Kalnay *et al.* (1981). These zonally asymmetric features attain a maximum in low latitudes, exhibiting an equivalent barotropic vertical structure with maximum amplitude near the tropopause.

A longitudinal phase versus time plot from daily analyses of zonal wavenumbers 4–7 (which contain the majority of the time variance) reveals periodic variations in both phase and amplitude: wave 5 frequently dominates, exhibiting eastward phase progression with period near 10 days. During other times, shorter scale waves (waves 6–7) exhibit enhanced amplitudes south and east of Africa, showing considerably faster eastward movement. Waves 6 and 7 both show remarkably regular eastward movement throughout the 90 day record, with periods near 5 and 4 days, respectively. The traveling waves exhibit maximum amplitude near the tropospheric jet core, often with an equivalent barotropic vertical structure.

The amplitude of the medium-scale waves is observed to vary with approximately the same time scale as the period of their phase progression (10–15 days). The zonal wind exhibits fluctuations of amplitude and time scale which suggest that the medium-scale waves may grow at the expense of the zonal mean kinetic energy. Episodes of latitudinal phase structure indicative of barotropic energy exchange with the mean wind field are observed. An exceptionally clear case of stationary-transient wave interference is observed.

1. Introduction

Analyses of data from the Global Weather Experiment conducted in 1979 are revealing new facets about atmospheric circulation. This note focuses on one such facet, viz., remarkable medium-scale waves which have been observed in Southern Hemisphere (SH) circulation patterns. These waves, which characteristically have about 5 wavelengths fitting around a latitude circle (wave 5), dominate both time mean and transient SH summer circulation patterns for the observation year.

The time mean waves were first noted in results from a global analysis with a 6-h forecast cycle, using Global Weather Experiment observations (Kalnay-Rivas *et al.*, 1981; Kalnay and Halem, 1981). Both time mean and traveling waves were found by Salby (1982) in SH NMC geopotentials derived from Global Weather Experiment data. Studying three months in the SH summer of 1978–79, Salby noted a maximum in the wavenumber spectrum at wave 5 and, additionally, a sharp peak in the time series spectrum corresponding to eastward propagation with period near 11 days.

Hamilton (1983) subsequently utilized Australian Bureau of Meteorology analyses to investigate the geopotential zonal wavenumber spectra at 300 and 500 mb for 1972–79 to determine if other years showed such unusual structures. In light of well-known pre-Global Weather Experiment inadequacies, Hamilton was surprised to find that waves 4–6 dominated the eddy fields for each of the 35 SH summer months he studied. Little evidence for similar phenomena was apparent in the SH winter. Analyses of EOLE balloon data by Desbois (1975) had revealed the existence of upper tropospheric kinetic energy maxima for waves 4–6 in the SH summer, while Adler (1977) found spectral peaks in this range for both SH summer and winter in analyses of Nimbus 3 infrared radiance measurements. Similar results were obtained by Kao *et al.* (1970) for both SH summer and winter from the study of IGY 500 mb height analyses. In agreement with Adler (1977), they also found these waves to be predominantly transient. Hartmann (1976) noted mid-tropospheric spectral peaks at wave 5 and periods of ~9 (and also 5) days from analyses of satellite retrievals during the SH winter of 1973. Due to the absence of winter wave 5 activity noted by Hamilton (1983), the

relationship between the above winter observations and the waves discussed here awaits further clarification.

In this note we point out several characteristics of the medium-scale waves during the SH summer 1978–79. In the time mean, features with typical horizontal wavelengths of 50–70° longitude are the dominant feature in low to middle latitudes. On a daily basis, waves 4–7 contain most of the variance throughout midlatitudes. Wave 5 frequently dominates with eastward phase progression with period near 10 days. Waves 6 and 7 also show regular eastward movement throughout the 90 day period. In addition, we observe variations in medium-scale wave amplitude with approximately the same periodicity as their phase progression. Episodes of barotropic interaction between the medium-scale waves and the mean zonal wind are also observed. One case is detailed in which these characteristics are clearly associated with stationary-transient wave interference.

2. Data analysis and results

a. Data and analysis technique

The data used in this investigation are the National Meteorological Center's daily SH analyses from 1 December 1978 to 28 February 1979 in the form of gridded geopotential height fields. Grids below 100 mb are NMC operational analyses. Geopotential heights at stratospheric levels are derived by converting the layer mean temperature (based on satellite and radiosonde data) to geopotential thickness and adding to the lower boundary at 100 mb. The satellite retrievals for this period were constructed from two operational satellite sounding systems: VTPR on NOAA 5 until 23 February 1979 and TOVS on TIROS-N thereafter.

Zonal and meridional geostrophic winds were calculated from the NMC grids, and then interpolated to a 2.5 × 2.5 degree latitude–longitude grid. The wind fields were then Fourier analyzed at each latitude to obtain amplitude and phase spectral components as a function of zonal wavenumber for each day. Infrequent missing days were filled by linear interpolation. Analysis of the winds on the NMC grids reveal a small area near the west coast of South America at low latitudes (15–25°S) where unreasonably large geostrophic winds result from several small scale irregularities in the grids. These points do not significantly alter the low-to-medium wavenumber Fourier components considered here; in addition, most of our attention is focused in midlatitudes. The wave kinetic energy is averaged latitudinally over the region 25–65°S and integrating vertically from 850 to 50 mb. This gives a better measure of features that have varying meridional and vertical profiles, and allows for comparisons with the zonal mean kinetic energy. In addition, the vertically integrated results are less sensitive to errors from satellite retrievals at specific pressure levels.

b. Spatial structure of the time-mean waves

Our investigation was originally motivated by the SH medium-scale time mean waves first observed by Kalnay *et al.* (1981). The presence of these waves is corroborated in our results; the January average meridional wind shown in Figs. 1a and 1b reveal that during summer 1978–79 the time mean fields at low to middle latitudes are dominated by medium-scale waves, with typical horizontal wavelengths of 50–70° longitude. (Fig. 1a has been smoothed by only retaining zonal wavenumbers $k \leqslant 12$, thus eliminating the low latitude irregularities mentioned above. The results were found to be insensitive to the exact wavenumber cutoff used. No smoothing was used in Fig. 1b.) In the seasonal mean 1 December 1978–28 February 1979, similar stationary features are evident, although of smaller amplitude (see bottom of Fig. 3). These time mean features are also observed in global grids of TIROS-N satellite microwave measurements which closely approximate the 30–150 mb geopotential thickness (Yu *et al.*, 1983).

The zonally asymmetric wave patterns seen in Fig. 1a show that no single zonal Fourier component can

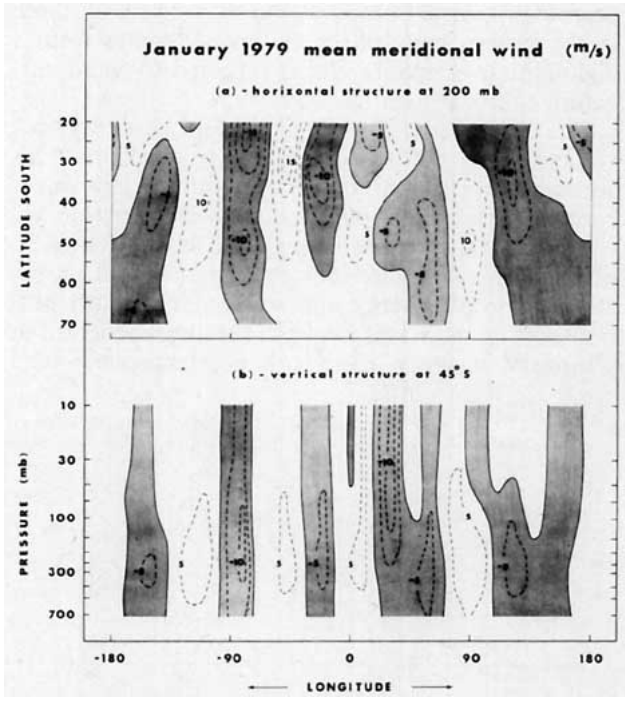

FIG. 1. Mean meridional geostrophic wind for January 1979. (a) Horizontal structure at 200 mb. (b) Vertical structure at 45°S. Shaded winds are southward.

accurately characterize these features, although wave 5 dominates the variance between 35° and 50°S. Rather, these features have the characteristics of localized wave packets, with the majority of the variance contained in wavenumbers 4–7. Fig. 2a shows the January time mean eddy kinetic energy in waves 4–7. The wave kinetic energy attains a maximum in the upper troposphere centered near 30°S, and decreases in altitude poleward, qualitatively similar to the behavior of the tropopause.

The wave patterns observed in Fig. 1a are similar to those produced by the barotropic dispersion of Rossby wave packets forced by localized planetary scale vorticity sources (Hoskins *et al.*, 1977). The waves in the eastern hemisphere exhibit a NW–SE tilt with latitude, a structure indicative of southward eddy momentum flux and wave energy propagation towards equatorial regions. The zonal group velocity of stationary Rossby waves is always eastward, and thus the group velocity vector here points from SW to NE.

Two groups of waves are evident in the western hemisphere. The largest amplitude waves are found in the South American region, with their phase being fairly constant with latitude over much of the amplified region. A second group with smaller amplitudes is found in the South Pacific ocean, where individual waves exhibit a more distinctive NE–SW tilt. This orientation indicates northward eddy momentum flux and wave energy propagation from equatorial to midlatitude regions. The group velocity vector here points from NW to SE. Note that energy in these waves appears to propagate from low latitudes, whereas for those in the eastern hemisphere the energy comes from a high-latitude source or else is reflected by wind curvature effects at high latitudes.

The vertical structure shown in Fig. 1b shows little vertical phase tilt throughout the troposphere. This allows the vertical structure to be termed equivalent barotropic, since the potential vorticity equation becomes separable in the vertical and horizontal coordinates. This structure indicates little vertical propagation of wave energy and small north–south heat transport by the waves, typical of features observed in stationary waves in the Southern Hemisphere (van

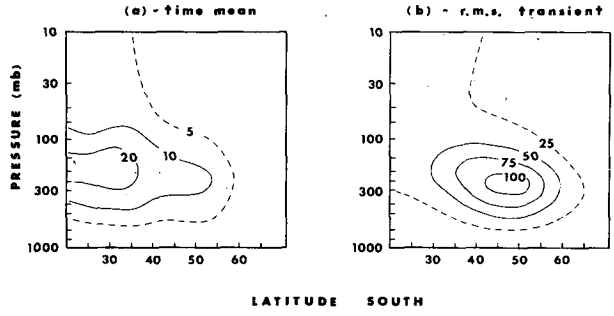

FIG. 2. Meridional sections of eddy kinetic energy ($m^2 s^{-2}$) for zonal wavenumbers 4–7. (a) January 1979 time mean. (b) January 1979 rms transient.

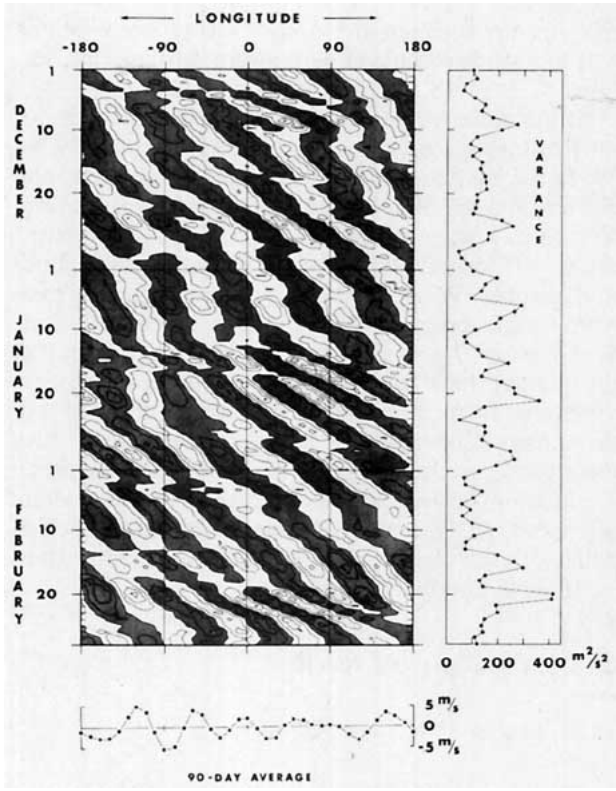

FIG. 3. Longitudinal phase versus time plot of the meridional geostrophic wind for zonal wavenumbers 4–7 at 200 mb and 45°S. Shaded winds are southward, with contour intervals of 10 m s^{-1}. Also shown is the associated variance versus time (right side), and 90-day average wave (bottom).

Loon and Jenne, 1972). In addition to these medium-scale features, a latitudinally and longitudinally narrow stratospheric maximum is observed south of Africa (near 30°E longitude).[1]

c. *Traveling waves*

On a daily basis the midlatitude wave activity is also dominated by medium-scale waves, as shown by Salby (1982). For this reason we restrict our attention to waves 4–7. Fig. 2b shows the January rms transient eddy kinetic energy in this wave band; note that the kinetic energy is centered in the upper troposphere near 45°S, poleward of the corresponding time mean features.

Figure 3 shows a longitude–time contour plot of the meridional wind at 45°S and 200 mb constructed with waves 4–7, illustrating the time variation of these waves. Wave 5 frequently dominates, exhibiting quasi-regular eastward phase progression with period near 10 days (eastward phase velocity near 6 m s^{-1}). This is in agreement with Salby (1982), who noted a sharp

[1] *Note added in proof.* The origin of this feature is unclear. It has been suggested (David Shaw, private communication) that it is due to a problem of data associated with Marion Island (°S, °E).

peak in the power spectra of wave 5 in this region near 11 days. Fig. 3 also shows that while slow phase progression is sometimes observed in the western hemisphere (where the largest time mean waves are observed), waves in the eastern hemisphere on occasion show more rapid movement (see, for example, the period 17–25 January). These regions of rapid movement are dominated by features with shorter zonal scales (waves 6–7). Fig. 4 shows that both wave 6 and 7 exhibit regular eastward phase progression throughout the 90-day period: wave 6 has period near 5 days (phase velocity 11 m s^{-1}), and wave 7 near 4 days (12 m s^{-1}). Again, these features are in good agreement with independent satellite microwave measurements (Yu *et al.*, 1983).

Although vertical phase tilts of 0.10–0.15 wavelength sometimes occur, our analyses reveal that, like the time-mean waves, the traveling wave 5 usually exhibits equivalent barotropic vertical structure (Fig. 5). Lines of constant phase frequently tilt substantially with latitude, indicating that the medium-scale waves are transporting momentum and exchanging energy barotropically with the zonal mean wind field. This will be discussed more fully in the next section.

d. Wave amplitude vacillation

Our analysis reveals that the amplitude of the medium-scale waves varies on the same time scale as the period of their phase progression (of order 10 days). This is exhibited in the variance shown in Fig. 3. Since these features have varying meridional profiles, a better measure of their amplitude maxima and minima is given by averaging the associated kinetic energy latitudinally and integrating vertically (see Section 2a). Fig. 6 shows the contributions to this kinetic energy from waves 4–7 individually, and shows that medium-scale wave amplitude maxima are frequently spread over several wavenumbers, suggesting wavepacket-like behavior. At other times, however, wave 5 appears to the exclusion of other wavenumbers (1–9 January and 7–12 February, for example), so that the circulation exhibits remarkable five-fold zonal symmetry.

When the kinetic energy of waves 4–7 is combined (bottom Fig. 7), amplitude maxima are observed semi-regularly with a time scale of 10–15 days. Seven of eight instances of wave amplitude maxima occur when the phase of wave 5 has approximately the same value (within the shaded region) as that of time-mean wave 5 (top Fig. 7). Hamilton (1983) also noted that the transient wave 5 amplitude frequently varied on the same time scale as its period. This correlation suggests two possible explanations for the semi-regular ap-

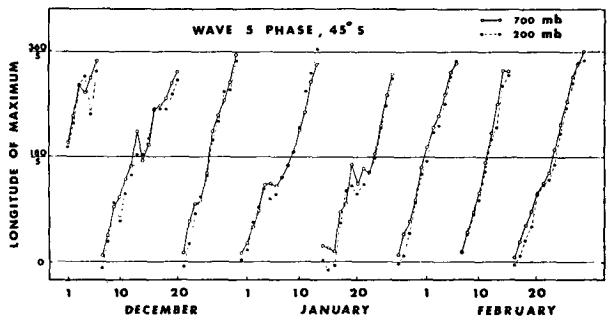

FIG. 5. Phase progression at 45°S for traveling wave 5 at 700 and 200 mb, showing the vertical tilt between these levels. The 90 day average wave has been subtracted from the daily values.

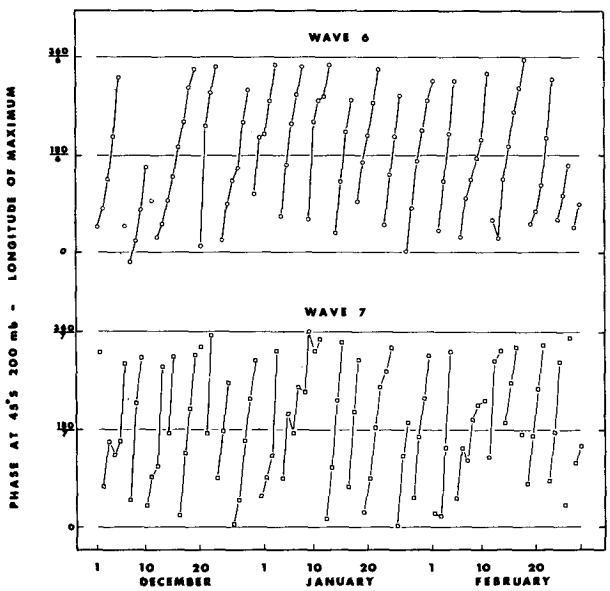

FIG. 4. Phase progression at 45°S for traveling waves 6 (top) and 7 (bottom) showing regular eastward phase progression with periods near 5 and 4 days, respectively. The 90 day average wave has been subtracted from the daily values in both cases.

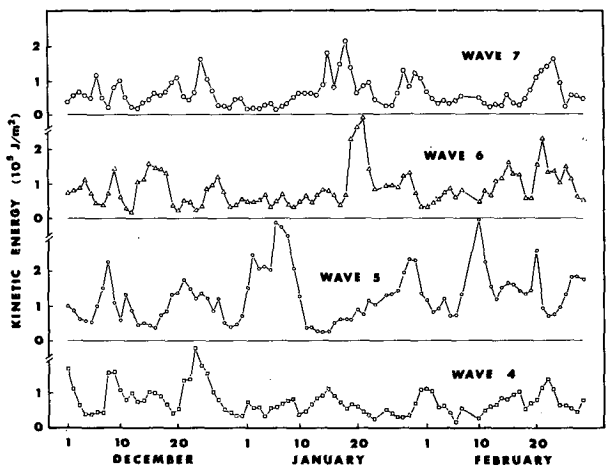

FIG. 6. Kinetic energy per unit area for zonal wavenumbers 4–7 individually during the SH summer 1978–79. The kinetic energy has been averaged latitudinally over 25°S to 65°S and integrated vertically from 850 to 50 mb.

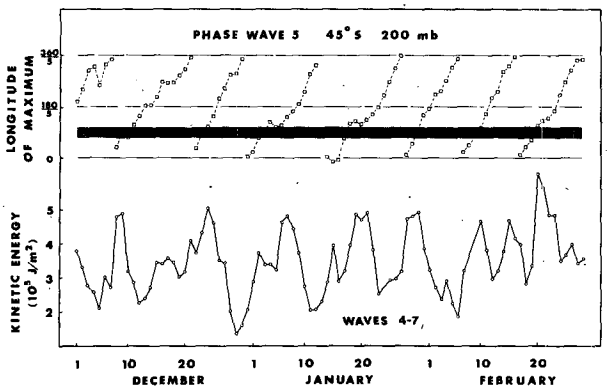

FIG. 7. Phase progression of traveling wave 5 at 200 mb and 45°S (top). Kinetic energy per unit area for waves 4–7 combined (bottom). In seven of eight cases the kinetic energy maxima occur when the traveling wave 5 is within the shaded region.

pearance of wave amplitude maxima: 1) standing wave/transient wave interference and/or 2) preferred region(s) of wave amplification. Both mechanisms would result in the correlation observed in Fig. 7, along with the presence of time-mean waves shown earlier.

An important clue to the origin of this behavior is that the zonal mean kinetic energy is sometimes observed to exhibit fluctuations with approximately the same amplitude and time scale as the medium-scale waves, as is shown in Fig. 8. The anti-correlations observed on occasion in Fig. 8 suggest that the medium-scale waves may grow and decay through energy exchanges with the zonal mean current. These energy exchanges are often found to be barotropic.

One exceptionally clear case of stationary transient wave interference is detailed here in the study of the growth and decay of the medium-scale waves during 30 December–11 January. Specifically, we observe barotropic wave-mean flow energy exchanges, commensurate mean flow kinetic energy changes, and a slowing of the phase progression of the wave.

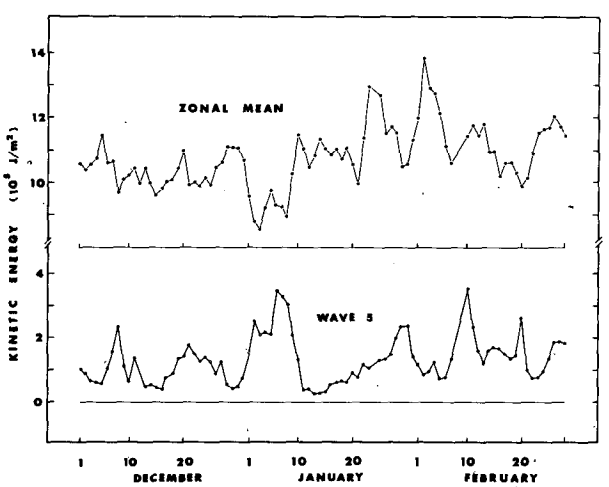

FIG. 8. Time variation of kinetic energy per unit area in the zonal mean (top) and wave 5 (bottom).

During 30 December–11 January a strong wave 5 appears to the exclusion of other wavenumbers, remaining nearly stationary for several days (see Fig. 3). Inspection of Fig. 8 during this time shows that the increase in wave 5 kinetic energy is approximately balanced by a decrease in zonal mean kinetic energy, and vice-versa. Fig. 9a (9b) shows an Eliassen–Palm diagram for wave 5 for 1 January (9 January) when the wave is growing (decaying). (For a review of the dynamical information available in an Eliassen-Palm diagram, see Edmon *et al.*, 1980. The plotting convention used here follows that in Dunkerton *et al.*, 1981.)

Linear wave interference between barotropic waves in a mean flow will produce barotropic wave-mean flow energy exchanges. Fig. 9a shows that the predominant wave fluxes in the upper troposphere are indeed barotropic (predominantly horizontal arrows) and that the effect of the wave 5 on the mean flow is largest in the region 30–50°S, near 250 mb. This is precisely the region where the largest overlap of the transient and stationary waves occurs (see Fig. 2a and 2b) and thus where the interaction is expected to be largest. Calculations show the northward potential vorticity gradient to be positive throughout this region (equatorward of the jet core), suggesting little likelihood of an instability in this region.

The structure of wave 5 on 9 January (Fig. 9b) shows nearly opposite wave characteristics throughout the same region, in excellent agreement with the interference hypothesis.

A decrease in zonal wind speed, caused by the above barotropic interactions, causes an apparent slowing down of the wave embedded in the flow. Calculations of the intensity of the jet core show a 7 m s^{-1} drop between 30 December and 3 January (33 m s^{-1} to 26 m s^{-1}) which, given the average 6 m s^{-1} phase speed of wave 5, agrees well with the near stationarity of the wave during this period.

The above results show that the wave amplitude maxima during this period can clearly be attributed to stationary–transient wave interference. While this is true for the 30 December–11 January case, other amplitude maxima observed in Fig. 7 do not exhibit such clear wave interference characteristics, thus making their identification less definitive.

3. Discussion

We have presented preliminary results on the space and time structure of medium-scale wave features which dominated the SH 1978–79 summer upper

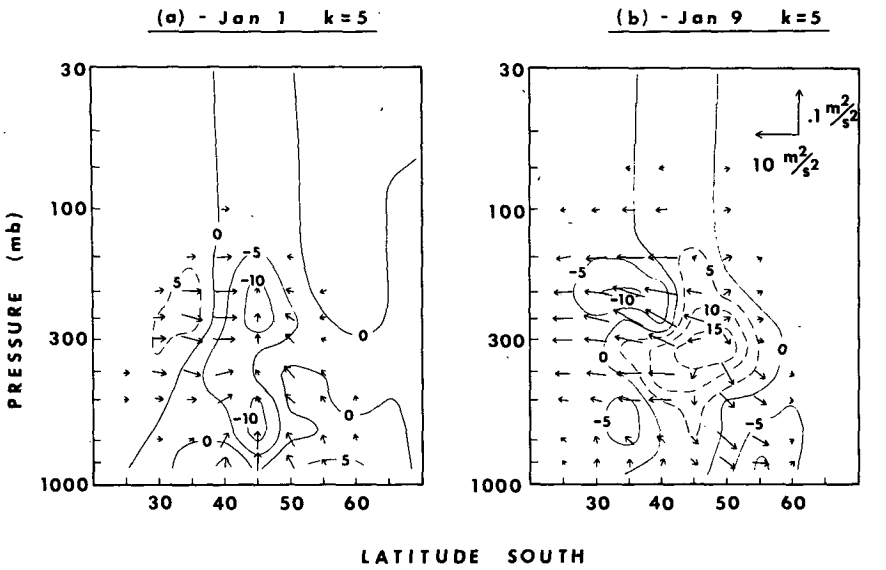

FIG. 9. Eliassen-Palm cross sections for zonal wavenumber 5 at beginning [(a) 1 January] and end [(b) 9 January] of an interference episode. The plotting convention used here follows that in Dunkerton *et al.* (1981). The arrow scales are given in the top right-hand corner of (b), with the horizontal and vertical components to be multiplied by $2\pi a^2 \rho_s$ and $2\pi a^3 \rho_s$, respectively. The contour interval is $2\pi a^3 \rho_s \times 5 \times 10^{-6}$ m s^{-2}.

tropospheric and lower stratospheric circulation, both for the time mean as well as traveling components. The results of several other authors mentioned in the Introduction indicate that medium-scale wave dominance is a common feature of the SH summer circulation.

As shown here and noted for other years, the waves are predominantly transient, although during the 1978–79 summer the time mean fields are also dominated by medium-scale features. In light of the results of van Loon and Jenne (1972) and Trenberth (1980), who reported primarily only standing waves 1–3 in the SH summer data they analyzed, it remains unclear the extent to which medium-scale wave domination is a recurrent circulation feature in years other than 1978–79. These time mean features are at least partly attributable to the fact that the transient waves become nearly stationary at times, although the different meridional profiles of the time-mean and transient-eddy kinetic energy (Figs. 2a and 2b) show that this is not the entire cause. The mechanism which maintains these low latitude features is not understood.

We have noted several intriguing characteristics of the medium-scale waves during this year, in particular their dominance and regular eastward phase progression throughout the summer. These aspects of the waves are more reminiscent of structures observed in laboratory annulus experiments (Pfeffer *et al.*, 1980) and observed on Mars (Barnes, 1980) than of any previously studied terrestrial features. A more thorough understanding of the unique features of the Southern Hemisphere atmosphere promises to shed valuable light on fundamental atmospheric processes.

Acknowledgments. This work has been supported jointly by the National Science Foundation under Grant ATM 79-11878, and the National Oceanic and Atmospheric Administration under Grant 81-21952. The geopotential data were generously supplied by M. E. Gelman of the Climate Analysis Center, National Oceanic and Atmospheric Administration. We wish to thank Dr. Mark Schoeberl for helpful discussions. One of us (WJR) has been supported by a L. H. Brown Trust Fellowship during a portion of this work.

REFERENCES

Adler, R. F., 1977: Characteristics of Southern Hemisphere 200-mb flow as determined from satellite data. *J. Geophys. Res.*, **82**, 427–432.

Barnes, J., 1980: Time spectral analysis of midlatitude disturbances in the Martian atmosphere. *J. Atmos. Sci.*, **37**, 2002–2015.

Desbois, M., 1975: Large-scale kinetic energy spectra from Eulerian analysis of EOLE wind data. *J. Atmos. Sci.*, **32**, 1838–1847.

Dunkerton, T., C.-P. F. Hsu and M. E. McIntyre, 1981: Some Eulerian and Lagrangian diagnostics for a model stratospheric warming. *J. Atmos. Sci.*, **38**, 819–843.

Edmon, H. J., Jr., B. J. Hoskins and M. E. McIntyre, 1980: Eliassen–Palm cross sections for the troposphere. *J. Atmos. Sci.*, **37**, 2600–2616.

Hamilton, K., 1983: Aspects of wave behavior in the mid and upper troposphere of the Southern Hemisphere. *Atmos. Ocean*, **21**, 40–54.

Hartmann, D. L., 1976: The structure of the stratosphere in the Southern Hemisphere during late winter 1973 as observed by satellite. *J. Atmos. Sci.*, **33,** 1141–1154.

Hoskins, B. J., A. J. Simmons and D. G. Andrews, 1977: Energy dispersion in a barotropic atmosphere. *Quart. J. Roy. Meteor. Soc.*, **103,** 553–567.

Kalnay, E., and M. Halem, 1981: Large amplitude stationary Rossby waves in the Southern Hemisphere. *Int. Conf. Early Results of FGGE and Large Scale Aspects of its Monsoon Experiments,* Tallassee, WMO, 3-5 to 3-15.

Kalnay-Rivas, E., W. Baker, M. Halem, R. Atlas and D. Edelmann, 1981: GLAS experiments with FGGE II-b data. *Proc. Int. Conf. Preliminary FGGE Data Analysis and Results,* Bergen, WMO, 150–161.

Kao, S.-K., R. L. Jenne and J. F. Sagendorf, 1970: The kinetic energy of large-scale atmospheric motion in wavenumber–frequency space. II: Mid-troposphere of the Southern Hemisphere. *J. Atmos. Sci.*, **27,** 1008–1020.

Pfeffer, R. L., G. Buzyna and R. Kung, 1980: Time-dependent modes of behavior of thermally driven rotating fluids. *J. Atmos. Sci.*, **37,** 2129–2149.

Salby, M. L., 1982: A ubiquitous wave 5 anomaly in the Southern Hemisphere during FGGE. *Mon. Wea. Rev.*, **110,** 1712–1720.

Trenberth, K. E., 1980: Planetary waves at 500 mb in the Southern Hemisphere. *Mon. Wea. Rev.*, **108,** 1378–1389.

van Loon, H., and R. L. Jenne, 1972: The zonal harmonic standing waves in the Southern Hemisphere. *J. Geophys. Res.*, **77,** 992–1003.

Yu, W.-B., R. L. Martin and J. L. Stanford, 1983: Long and medium-scale waves in the lower stratosphere from satellite-derived microwave measurements. *J. Geophys. Res.* (in press).